Supporting Information

Substrate-to-Product Conversion Facilitates Active Site Loop Opening in Yeast Enolase: A Molecular Dynamics Study

Pengfei Li and Sharon Hammes-Schiffer*

Department of Chemistry, Yale University, 225 Prospect Street,
New Haven, Connecticut 06520

*sharon.hammes-schiffer@yale.edu

TABLE OF CONTENTS

Protocol for System Preparation

Yeast enolase is a protein dimer with each monomer consisting of 436 amino acid residues. In the PDB entry 1ONE,[1] yeast enolase is crystalized with the substrate 2-phosphoglyceric acid (2PG) and product phosphoenolpyruvate (PEP). These structures were used to model the protein-ligand complexes. The H++ webserver[2] was utilized to determine the protonation states of the amino acid residues. Because H++ does not consider metal ions, water molecules, or ligands, we adjusted the protonation states of some amino acids in the active site. For the protein-2PG system, we adjusted Hie159 to Hip159, Glu211 to Glh211, Ash246 to Asp246, Glh295 to Glu295, and Lys345 to Lyn345 in Chain A, as well as Hie159 to Hip159, Glu211 to Gln211, Ash246 to Asp246, and Lys345 to Lyn345 in Chain B. For the protein-PEP system, we adjusted Hie159 to Hip159, Ash246 to Asp246, and Glh295 to Glu295 in Chain A, as well as Hie595 to Hip595 and Ash246 to Asp246 in Chain B. These three-letter residue names use the AMBER naming scheme based on the protonation states. In the remaining parts of the SI, the naming scheme of the residues is consistent with that in the PDB (e.g., His159 instead of Hip159).

Force Field Parameters

For both 2PG and PEP, the triply deprotonated form was used with a total charge of –3, and the enol intermediate was assigned a total charge of –4. The partial charges for these ligands were determined in a manner consistent with the AMBER force field. The structure of 2PG/PEP was optimized at the HF/6-31G* level of theory. At the same level of theory, the enol intermediate was first optimized with the three carbon atoms fixed, followed by a full optimization. The Mulliken population analysis and Merz-Kollman population analysis were performed at the same level of theory based on these optimized geometries. Finally, the RESP charges were fitted based on the population analysis using the two-stage RESP algorithm. The Gaussian09 program[3] was used for these quantum mechanical calculations, and the antechamber module in the AMBER software package[4] was utilized for the RESP fitting. The RESP charges were used in the simulations. The RESP charges, Mulliken charges, and atom types of the 2PG, enol intermediate, and PEP are given in Table S1.

The crystal waters were retained for the protein-ligand complexes, and a cuboid water box of ~113×107×94 Å was used to solvate each of the complexes, ensuring that the distance from the protein surface atoms to the box edge was at least 12 Å. The TIP3P water model[5] was used to represent the solvent. 87 Na^+ and 87 Cl^- ions were added to the system as counterions to provide a salt concentration of ~0.15 M for the molecular dynamics (MD) simulations. The van der Waals (VDW) parameters of the Mg^{2+} ions were obtained from the compromise (CM) parameter set designed for the TIP3P water model,[6] and the VDW parameters of the Na^+ and Cl^- ions were obtained from the hydration free energy (HFE) parameter set designed for the TIP3P water model.[7] The ff14SB force field[8] was used to model the protein-ligand complexes, with additional parameters for the PEP ligand given below.

```
MASS
CE 12.010       0.360
CF 12.010       0.360

BOND
C -CE  410.00   1.444      same as  C-CM
CE-CF  549.00   1.350      same as CM-CM
CE-OS  480.00   1.240      same as CM-OS
CF-HA  367.00   1.080      same as CM-HA

ANGLE
C -CE-CF   63.000     120.000   force constant same as C -CM-CM
C -CE-OS   80.000     120.000   force constant same as CM-CM-OS
CF-CE-OS   80.000     120.000   force constant same as CM-CM-OS
CE-C -O2   80.000     120.000   force constant same as CM-C -O
CE-CF-HA   50.000     120.000   force constant same as CM-CM-HA
HA-CF-HA   35.000     120.000   force constant same as HA-CM-HA
CE-OS-P   100.000     120.500   same as C -OS-P

DIHE
C -CE-OS-P    2    1.800      180.000         2.000      same as X -CA-OH-X
O2-C -CE-CF   1    2.175      180.000        -2.000      same as CM-CM-C -O
O2-C -CE-CF   1    0.300        0.000         3.000      same as CM-CM-C -O
O2-C -CE-OS   4   14.500      180.000         2.000      same as X -C -CA-X
CF-CE-OS-P    2    1.800      180.000         2.000      same as X -CA-OH-X
OS-CE-CF-HA   4   26.600      180.000         2.000      same as X -CM-CM-X
C -CE-CF-HA   4   26.600      180.000         2.000      same as X -CM-CM-X
CE-OS-P -O2   3    0.750        0.000         3.000      same as X -OS-P -X

IMPROPER
CE-O2-C -O2       10.5        180.0       2.0        Using general improper torsional angle  X-O2- C-O2
C -CF-CE-OS        1.1        180.0       2.0        Using the default value
CE-HA-CF-HA        1.1        180.0       2.0        Using the default value

NONBON
  CE          1.9080  0.0860
  CF          1.9080  0.0860
```

Protocol for Molecular Dynamics Simulations

The following procedures were performed for both the protein-2PG and protein-PEP complexes.

(A) Equilibration of the solvent, counter-ions, and protein hydrogen atoms

First, the following three steps were carried out to equilibrate the solvent, counter-ions, and hydrogen atoms in the protein-ligand complex:
(1) 10000 steps of minimization with the steepest descent algorithm;
(2) 500 ps NVT equilibration at 300 K;
(3) 500 ps NPT equilibration at 300 K and 1 atm.
During these three steps, 200 kcal/(mol•Å^2) restraints were applied to the heavy atoms in the protein-ligand complex (including the Mg^{2+} ions). A 1 fs time-step was used for the NVT and NPT simulations.

(B) Relaxation of the complex

After the initial solvent equilibration, five steps of minimization were carried out to gradually relax the protein-ligand complex:
(4) 10000 steps of minimization using the steepest descent algorithm followed by 10000 steps of minimization using the conjugated gradient algorithm. This step of minimization has 100 kcal/(mol•Å^2) restraints on the heavy atoms of the protein-ligand complex (including the Mg^{2+} ions).
(5) 10000 steps of minimization using the steepest descent algorithm followed by 10000 steps of minimization using the conjugated gradient algorithm. This step of minimization has 100 kcal/(mol•Å^2) restraints on the C, C_α, and N atoms of the protein.
(6) 10000 steps of minimization using the steepest descent algorithm followed by 10000 steps of minimization using the conjugated gradient algorithm. This step of minimization has 50 kcal/(mol•Å^2) restraints on the C, C_α, and N atoms of the protein.
(7) 10000 steps of minimization using the steepest descent algorithm followed by 10000 steps of minimization using the conjugated gradient algorithm. This step of minimization has 10 kcal/(mol•Å^2) restraints on the C, C_α, and N atoms of the protein.
(8) 10000 steps of minimization using the steepest descent algorithm followed by 10000 steps of minimization using the conjugated gradient algorithm. This step of minimization does not have any restraints.

(C) Heating and equilibration

The following steps were carried out to heat and equilibrate the system:
(9) 360 ps NVT heating was carried out to gradually heat the system from 0 to 300 K:

(a) 10 ps simulation to heat the system from 0 to 50 K, followed by 50 ps simulation to equilibrate the system at 50 K;

(b) 10 ps simulation to heat the system from 50 to 100 K, followed by 50 ps simulation to equilibrate the system at 100 K;

(c) 10 ps simulation to heat the system from 100 to 150 K, followed by 50 ps simulation to equilibrate the system at 150 K;

(d) 10 ps simulation to heat the system from 150 to 200 K, followed by 50 ps simulation to equilibrate the system at 200 K;
(e) 10 ps simulation to heat the system from 200 to 250 K, followed by 50 ps simulation to equilibrate the system at 250 K;
(f) 10 ps simulation to heat the system from 250 to 300 K, followed by 50 ps simulation to equilibrate the system at 300 K.

(10) After this initial heating, 2 ns NPT simulation was carried out at 300 K and 1 atm to further equilibrate the system and correct the density.

(D) Production simulation

(11) Finally, 1.02 μs NVT simulation at 300 K was carried out for production. The configurations were saved every 10 ps, and this trajectory was used for data analysis. A 2 fs time-step was used for the simulations in Steps 9-11.

Periodic boundary conditions were employed for all of the minimizations and MD simulations. The nonbonded cut-off was set to 10 Å, and the particle mesh Ewald (PME) method[9] was used to treat the long-range electrostatic interactions. A Langevin thermostat with a collision frequency of 2 ps^{-1} was employed to control the temperature in the MD simulations, and a Berendsen barostat was utilized to control the pressure in the NPT simulations. The SHAKE algorithm[10] was used to constrain the bond lengths involving hydrogen atoms in the MD simulations, except that a specific "three-point" SHAKE algorithm[11] was used for the water molecules. The minimizations and MD simulations were carried out by the pmemd.cuda program[12] in Amber16.[13-14] All of the restraints in these simulations were based on the equation $U(r)=k(r-r_0)^2$, where k is the restraint strength and r_0 is the equilibrium bond length. The same conditions stated in this paragraph were used for the umbrella sampling simulations discussed below.

Protocol for Umbrella Sampling Simulations

The umbrella sampling simulations for the protein-2PG and protein-PEP systems were performed according to the following procedure. Note that that the umbrella restraints were applied only to Chain A of each system during these simulations, while Chain B was free to move.

(A) Equilibration of the windows

As stated in the main text, two reaction coordinates, which correspond to the distance between Mg_B^{2+} and Ser39C_α and the distance between Ala38O and Glu47N, were used to generate the free energy surfaces. The closed loop state was characterized by (3.5 Å, 11.5 Å), and the open loop state was characterized by (13.58 Å, 2.86 Å), where the first and second values correspond to the first and second reaction coordinates, respectively. During the two-dimensional scan, the X axis has 25 windows of range 3.5–13.58 Å with an interval of 0.42 Å, and the Y axis has 35 windows of range 2.86–15.10 Å with an interval of 0.36 Å, which provides a total of 875 windows. The equilibration for these windows was performed in a similar manner as described in Figure S2 in the Supporting Information of a previous publication.[15]

First the 25 windows along the diagonal (from the closed loop state to the open loop state) were scanned in the following way. The structure after NPT equilibration in Step 10 of the procedure described above was used as the initial structure for the closed loop state. Then 1 ns umbrella sampling simulation was performed to equilibrate the system with the restraints for the first window. The final configuration from the first window was used as the initial structure for the second window along the diagonal, and 1 ns umbrella sampling simulation was performed for the second window. Then the final configuration of the second window was used as the initial structure for the third window. This cycle continued until completing the 1 ns umbrella sampling simulations for all 25 windows.

After finishing the scan along the diagonal, a scan along the Y axis from windows on the diagonal was carried out as depicted in the Figure S2b in the Supporting Information of the previous publication.[15] At the end of this procedure, each of the 875 windows had 1 ns equilibration, and the final configuration of each window was used in the umbrella sampling simulations described below. In these equilibration simulations, 50 kcal/(mol*Å^2) restraints were applied to both reaction coordinates with the equilibrium distances given above.

(B) Umbrella sampling simulations

The umbrella sampling simulations started from the equilibrated structures of the 875 windows. During these simulations, 10 kcal/(mol*Å^2) restraints were applied to both reaction coordinates with the same equilibrium distances used in the equilibration procedure. For each of the 875 windows, 4 sequential umbrella sampling simulations, each of length 1 ns, were performed. The values of the reaction coordinates were saved every 10 fs. To enhance the sampling efficiency, the atomic velocities were reassigned at the beginning of each 1 ns simulation. Within each 1 ns simulation, the first 200 ps was treated as equilibration, and the last 800 ps was used to generate the final free energy profile.

(C) Generation of the free energy profiles

The umbrella sampling results were unbiased to obtain the two-dimensional free energy profile using the weighted histogram analysis method (WHAM).[16] For each system, 2.8 μs data (875*4*800 ps) was used to generate the free energy profile. During the WHAM analysis, the range of the X axis was set as 2.5–14.5 Å with 30 bins, and the range of the Y axis was set as 2.5–16.0 Å with 40 bins, while the temperature was set as 300 K, and the convergence tolerance was set as 0.001.

(D) Hydrogen-bonding analysis of L1 and the ligands in the closed loop and open loop states

The closed loop and open loop states for protein-2PG were estimated as (3.50 Å, 11.44 Å) and (9.50 Å, 9.76 Å) according to the free energy profile shown in Figure 5. In order to compare the hydrogen-bonding interactions involving loop L1 and the ligand in the two different states, we performed hydrogen-bonding analyses on the representative windows in the umbrella sampling simulations for the closed and open loop states. The four neighboring windows (3.50 Å, 11.14 Å), (3.50 Å, 11.5 Å), (3.92 Å, 11.14 Å), and (3.92 Å, 11.5 Å) were chosen to represent the closed loop state, while the four neighboring windows (9.38 Å, 9.70 Å), (9.38 Å, 10.06 Å), (9.80 Å, 9.70 Å), and (9.80 Å, 10.06 Å) were chosen to represent the open loop state. As mentioned above, for each window, 4 ns of MD was propagated with new velocities selected every 1 ns. For each of these 1 ns intervals, the last 80 snapshots, which were saved every 10 ps, were used for analysis, providing 1280 snapshots for each of the two states. The same procedure was performed for the protein-PEP system. The closed and open loop states for the protein-PEP system were estimated as (4.30 Å, 11.11 Å) and (10.70 Å, 7.06 Å), respectively. The four neighboring windows (3.92 Å, 10.78 Å), (3.92 Å, 11.14 Å), (4.34 Å, 10.78 Å), and (4.34 Å, 11.14 Å) were chosen to represent the closed loop state, while the four neighboring windows (10.64 Å, 6.82 Å), (10.64 Å, 7.18 Å), (11.06 Å, 6.82 Å), and (11.06 Å, 7.18 Å) were chosen to represent its open loop state. The results of these analyses are shown in Tables S7 and S8.

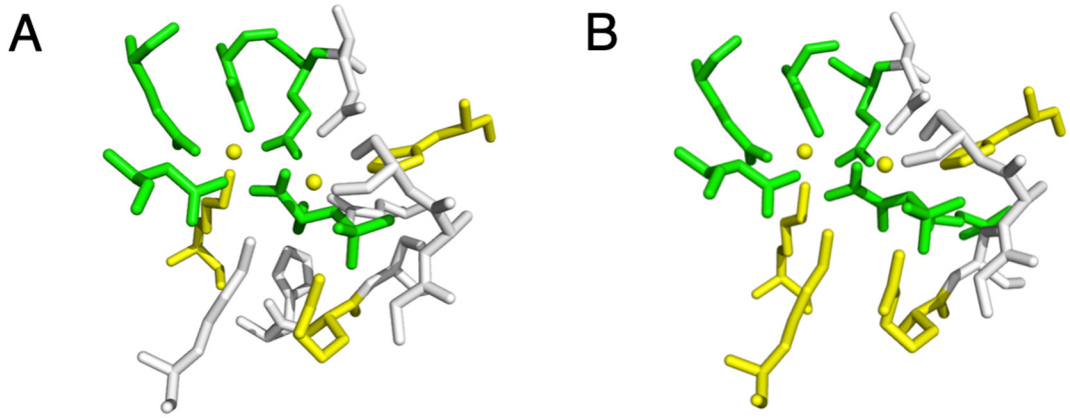

Figure S1. The active site residues that are within 3 Å of the ligand (A) in the reactant state and (B) in the product state. The positively charged residues and Mg^{2+} ions are colored yellow, the negatively charged residues and ligands are colored green, and the neutral residues are colored white. The structure is from Chain A of PDB entry 1ONE.[1]

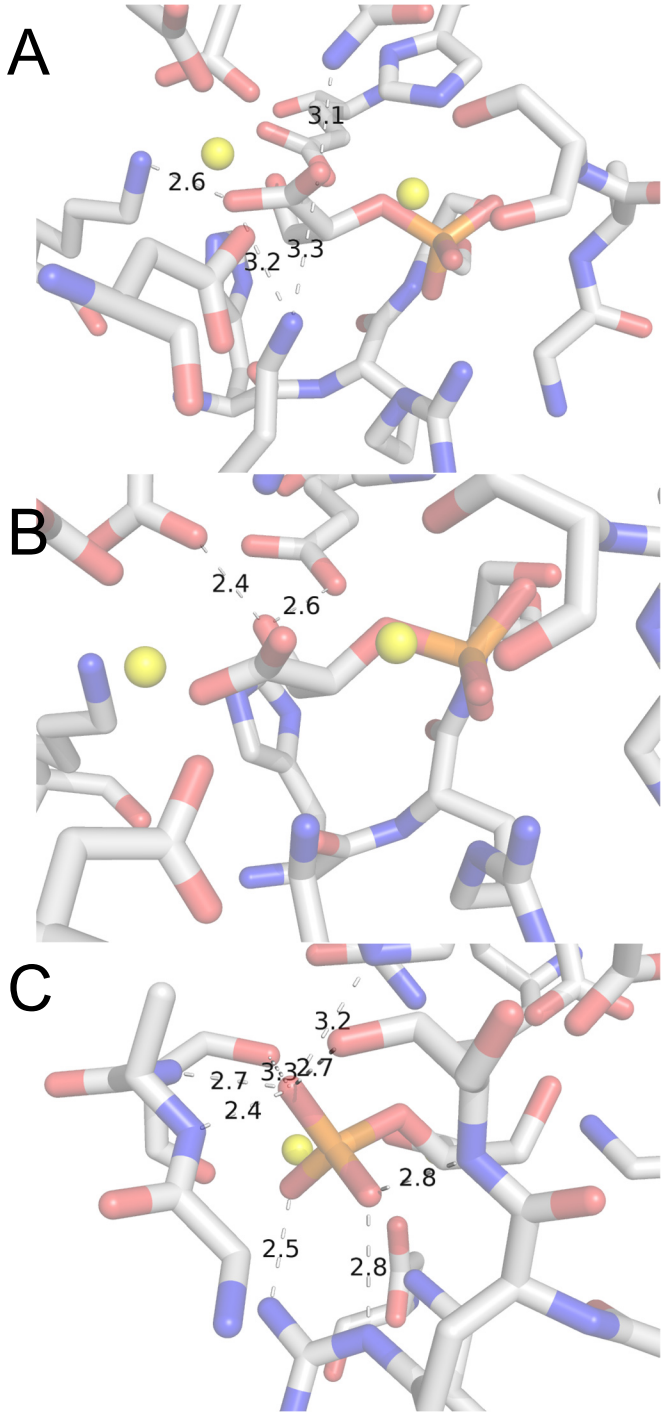

Figure S2. Potential hydrogen bonds between the yeast enolase and the 2PG substrate. The potential hydrogen bonds (A) between yeast enolase and the carboxylate group of 2PG, (B) between yeast enolase and the hydroxyl group of 2PG, and (C) between yeast enolase and the phosphate group of 2PG. The potential hydrogen bonds are represented by red dashed lines. The structure is from Chain A of PDB entry 1ONE,[1] and Chain B has a similar structure. The distances of these potential hydrogen bonds are given in Table S2.

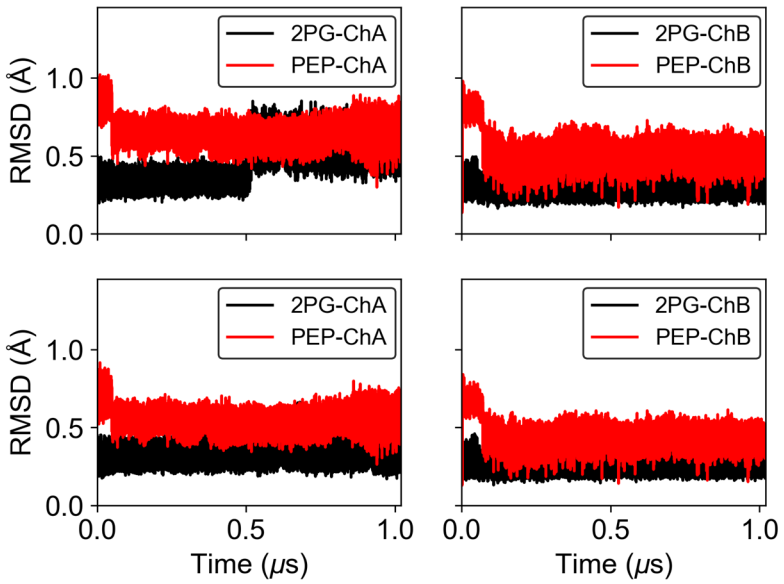

Figure S3. RMSDs of the heavy atoms in the ligand along the MD trajectories, relative to the crystal structure. Results of Chains A and B are depicted separately and are denoted ChA and ChB, respectively. To ensure a consistent comparison between 2PG and PEP, the hydroxyl group oxygen atom of 2PG was excluded when calculating all of these RMSDs. The lower panels differ from the upper panels in that the carboxylate oxygen atoms are excluded when calculating the RMSDs for the lower panels. Excluding the carboxylate oxygen atoms eliminates the jump at around 0.5 μs in the RMSD plot for 2PG in Chain A, which is mainly caused by rotation of the carboxylate group.

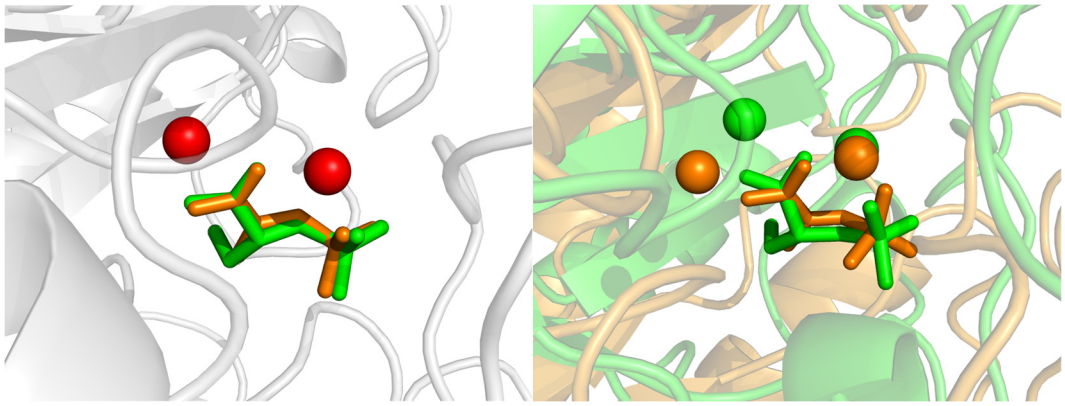

Figure S4. (Left) Substrate and product from Chain A of crystal structure 1ONE. The 2PG and PEP are depicted in green and orange, respectively, and the two Mg^{2+} ions are represented by red spheres. The protein has the same coordinates in this PDB entry for bound 2PG and PEP. (Right) Overlay of the substrate and product structures shown in Figure 2, corresponding to configurations at 360 ns in the production MD trajectories. The structures were superimposed by aligning the ligand heavy atoms excluding the C2 and hydroxyl oxygen atoms. The protein-2PG and protein-PEP systems are depicted in green and orange, respectively. Note that these are two representative configurations, and conformational fluctuations will occur through the MD trajectories (Figure S3).

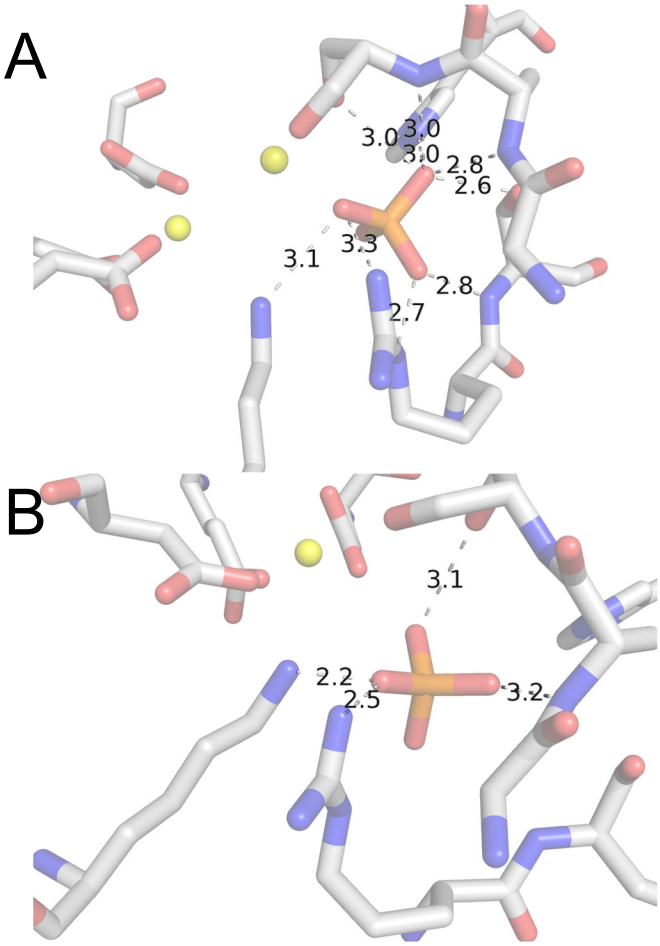

Figure S5. (A) Active site structure from chain A of PDB entry 2AKM, which corresponds to the E-Mg_A^{2+}-L-Mg_B^{2+} state, and (B) active site structure from chain B of PDB entry 2AKM, which corresponds to the E-Mg_A^{2+}-L state. Here L denotes the ligand, which is phosphate. The potential hydrogen bonds, defined in terms of heavy atom distances less than 3.30 Å, between the ligand and protein are shown with black dashed lines and red labels for the distances.

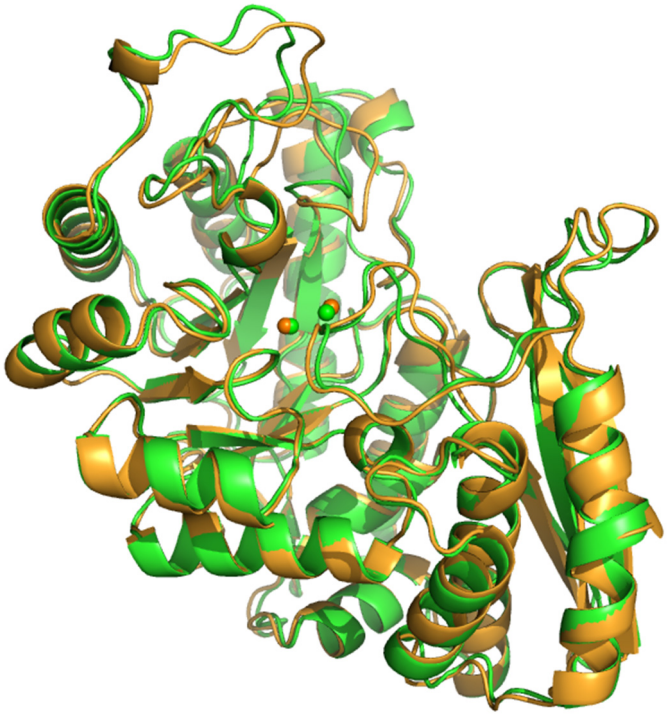

Figure S6. Overlay of the Chain A structure of PDB entry 1L8P (green) and a chosen configuration from the protein-PEP umbrella sampling simulation (orange). The alignment was performed by aligning the C_α atoms in Chain A. Chain A in PDB entry 1L8P has the two reaction coordinates as (6.08 Å, 11.72 Å). The chosen configuration was obtained at 940 ps during the first 1 ns umbrella sampling for the window with restraints corresponding to (6.02 Å, 11.5 Å), and the configuration itself has the two reaction coordinates as (6.04 Å, 11.67 Å).

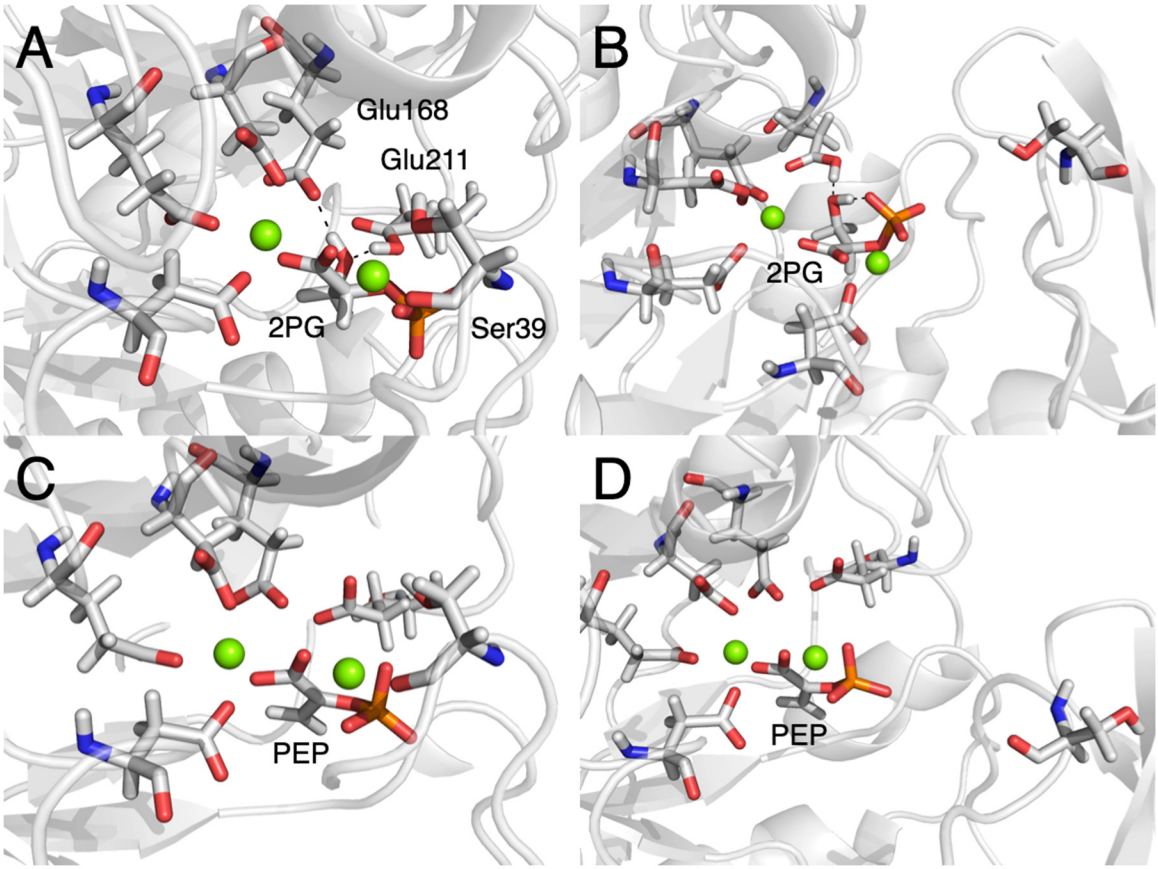

Figure S7. Representative binding modes of the substrate and product in the closed loop and open loop states: (A) substrate in the closed loop state; (B) substrate in the open loop state; (C) product in the closed loop state; (D) product in the open loop state. These structures were obtained from the configurations at 0.21 ns in the third 1 ns subsequent sampling of the windows (3.50 Å, 11.50 Å) and (9.38 Å, 9.70 Å) for the protein-2PG system, and of the windows (4.34 Å, 11.14 Å) and (10.64 Å, 7.18 Å) for the protein-PEP system. The hydrogen bonds involving the hydroxyl group of 2PG are indicated with dashed lines.

Table S1. Atom types, RESP charges, and Mulliken charges of the substrate, enol intermediate, and product[a]

2PG (substrate)							
Atom name	Atom type	RESP Charge	Mulliken Charge	Atom name	Atom type	RESP Charge	Mulliken Charge
C1	C	0.927161	0.693864	O2P	O2	-0.948220	-0.981586
C2	CT	0.264013	0.167064	O3P	O2	-0.948220	-0.954652
C3	CT	0.252432	-0.026932	O4P	O2	-0.948220	-0.918057
P	P	1.318940	1.481100	H32	H1	-0.049941	0.116852
O1	O2	-0.915723	-0.771641	H31	H1	-0.049941	0.095721
O2	O2	-0.915723	-0.841339	H3	HO	0.436742	0.511917
O3	OH	-0.757141	-0.866517	H2	H1	-0.094533	0.087935
O1P	OS	-0.571627	-0.793729				
Enol intermediate							
Atom name	Atom type	RESP Charge	Mulliken Charge	Atom name	Atom type	RESP Charge	Mulliken Charge
C1	C	1.102792	0.697452	O2P	O2	-1.030014	-1.000392
C2	CM	-0.785172	-0.054630	O3P	O2	-1.030014	-0.986719
C3	CT	0.256766	0.007311	O4P	O2	-1.030014	-1.013274
P	P	1.362572	1.434098	H32	H1	-0.025009	0.062939
O1	O2	-1.028535	-0.905652	H31	H1	-0.025009	0.046264
O2	O2	-1.028535	-0.966095	H3	HO	0.367719	0.464414
O3	OH	-0.777476	-0.932113				
O1P	OS	-0.330071	-0.853602				
PEP (product)							
Atom name	Atom type	RESP Charge	Mulliken Charge	Atom name	Atom type	RESP Charge	Mulliken Charge
C1	C	0.824740	0.662477	P	P	1.341127	1.458474
O1	O2	-0.870782	-0.817430	O1P	O2	-0.954477	-0.939942
O2'	O2	-0.870782	-0.773870	O2P	O2	-0.954477	-0.926629
C2	CE	0.437457	0.423458	O3P	O2	-0.954477	-0.950298
C3	CF	-0.847464	-0.575599	H32	HA	0.185055	0.161409
O2	OS	-0.520974	-0.796655	H31	HA	0.185055	0.074603

[a]These atom names are from the crystal structure PDB file. Because the crystal structure does not contain the enol intermediate, we used the atom names for the 2PG ligand for the enol intermediate as well. To facilitate discussion, the nomenclature for the oxygen atoms in 2PG and PEP used throughout the manuscript and other parts of the SI is clarified in Table S2. Note that the enol intermediate was not simulated in the molecular dynamics simulations, and its parameters are listed below only for illustration purpose.

Table S2. The charged residues in the active site of yeast enolase

Protein-2PG		Protein-PEP	
Residue	Charge	Residue	Charge
Glu168	-1	Glu168	-1
Glu211	0	Glu211	-1
Lys396	+1	Lys396	+1
Asp246	-1	Asp246	-1
Glu295	-1	Glu295	-1
Asp320	-1	Asp320	-1
Lys345	0	Lys345	+1
2PG	-3	PEP	-3
His159	+1	His159	+1
Arg374	+1	Arg374	+1
Mg_A^{2+}	+2	Mg_A^{2+}	+2
Mg_B^{2+}	+2	Mg_B^{2+}	+2
Total Charge	0	Total Charge	0

Table S3. Potential hydrogen bonds between yeast enolase and the ligand[a]

		2PG		PEP	
Acceptor[b]	Donor	Chain A	Chain B	Chain A	Chain B
O1	Lys345N$_\zeta$	3.3	3.3	3.3	3.3
O1	Gln167N$_{\varepsilon 2}$	3.1	3.0	3.1	3.1
O2	Lys345N$_\zeta$	3.2	3.2	3.0	2.9
O2	Lys396N$_\zeta$	2.6	2.6	2.8	2.8
Glu168O$_{\varepsilon 2}$	OH[b]	2.4	2.5	N/A	N/A
OH	Glu211O$_{\varepsilon 2}$	2.6	2.7	N/A	N/A
O$_A$	Arg374N$_{\eta 2}$	2.5	2.5	2.7	2.7
O$_B$	Ala38N	2.4	2.4	2.6	2.6
O$_B$	Ser39N	2.7	2.8	2.9	3.0
O$_B$	Ser39O$_\gamma$	3.3	3.5	3.3	3.4
O$_B$	His159N$_{\varepsilon 2}$	3.2	3.2	3.1	3.1
O$_B$	Ser375O$_\gamma$	2.7	2.5	2.7	2.5
O$_C$	Arg374N$_\varepsilon$	2.8	2.8	2.8	2.8
O$_C$	Ser375N	2.8	2.7	2.8	2.8

[a]These values are based on PDB entry 1ONE,[1] and the distances are given in units of Å.
[b]To facilitate discussion, this nomenclature of the oxygen atoms in the ligand, which is different from the crystal structure, is used in the main text and SI unless otherwise specified. Compared to 2PG, PEP has the same nomenclature for these atoms except that it does not have the hydroxyl group.

Table S4. Select average distances in the active site for the MD simulations of the protein-2PG and protein-PEP systems[a]

Protein-2PG					
Chain A			Chain B		
Atom 1	Atom 2	Distance	Atom 1	Atom 2	Distance
Mg_A^{2+}	μO of 2PG	2.65±0.45	Mg_A^{2+}	μO of 2PG	2.71±0.21
Mg_B^{2+}	μO of 2PG	1.92±0.05	Mg_B^{2+}	μO of 2PG	1.90±0.04
Mg_A^{2+}	Mg_B^{2+}	4.03±0.26	Mg_A^{2+}	Mg_B^{2+}	4.21±0.19
Mg_B^{2+}	O_A of 2PG	1.90±0.05	Mg_B^{2+}	O_A of 2PG	1.88±0.04
Mg_B^{2+}	O_B of 2PG	3.95±0.31	Mg_B^{2+}	O_B of 2PG	3.81±0.11
Mg_B^{2+}	O_C of 2PG	4.25±0.14	Mg_B^{2+}	O_C of 2PG	4.30±0.06
Mg_B^{2+}	Ser39O_γ	3.25±1.00	Mg_B^{2+}	Ser39O_γ	2.21±0.11
Lys345N_ζ	O_A of 2PG	3.34±0.39	Lys345N_ζ	O_A of 2PG	3.89±0.23
Lys345N_ζ	O_B of 2PG	5.65±0.34	Lys345N_ζ	O_B of 2PG	6.03±0.20
Lys345N_ζ	O_C of 2PG	4.52±0.43	Lys345N_ζ	O_C of 2PG	4.61±0.24
Protein-PEP					
Chain A			Chain B		
Atom 1	Atom 2	Distance	Atom 1	Atom 2	Distance
Mg_A^{2+}	μO of PEP	3.34±0.51	Mg_A^{2+}	μO of PEP	3.77±0.23
Mg_B^{2+}	μO of PEP	1.96±0.06	Mg_B^{2+}	μO of PEP	1.93±0.05
Mg_A^{2+}	Mg_B^{2+}	5.07±0.56	Mg_A^{2+}	Mg_B^{2+}	5.37±0.27
Mg_B^{2+}	O_A of PEP	1.90±0.04	Mg_B^{2+}	O_A of PEP	1.90±0.04
Mg_B^{2+}	O_B of PEP	4.26±0.13	Mg_B^{2+}	O_B of PEP	4.28±0.15
Mg_B^{2+}	O_C of PEP	3.26±0.33	Mg_B^{2+}	O_C of PEP	3.38±0.38
Mg_B^{2+}	Ser39O_γ	4.34±1.32	Mg_B^{2+}	Ser39O_γ	4.17±0.62
Lys345N_ζ	O_A of PEP	4.78±0.22	Lys345N_ζ	O_A of PEP	4.86±0.12
Lys345N_ζ	O_B of PEP	4.89±0.15	Lys345N_ζ	O_B of PEP	4.67±0.16
Lys345N_ζ	O_C of PEP	2.75±0.10	Lys345N_ζ	O_C of PEP	2.71±0.12

[a]These distances are represented by the average values followed by standard deviations.

Table S5. Statistics associated with the hydrogen bonds between the phosphate and hydroxyl groups of the ligand and the protein residues for the MD simulations of the protein-2PG and protein-PEP systems[a]

Chain A					
Protein-2PG			Protein-PEP		
Acceptor	Donor	Percentage	Acceptor	Donor	Percentage
Glu168$O_{\varepsilon1/\varepsilon2}$	OH of 2PG	81.5%	N/A		
OH of 2PG	Glu211$O_{\varepsilon2}$	52.6%	N/A		
OH of 2PG	His159$N_{\varepsilon2}$	16.6%	N/A		
O_A of 2PG	Arg374$N_{\eta2}$	74.8%	O_A of PEP	His159$N_{\varepsilon2}$	14.1%
O_B of 2PG	Ser39N	94.6%	O_A of PEP	Ser39O_γ	12.5%
O_B of 2PG	Ser39O_γ	93.6%	O_B of PEP	Ser375N	77.8%
O_B of 2PG	His159$N_{\varepsilon2}$	60.4%	O_B of PEP	Arg374N_ε	57.9%
O_B of 2PG	Ala38N	50.4%	O_B of PEP	Ser375O_γ	24.9%
O_B of 2PG	Ser375O_γ	35.2%	O_C of PEP	Lys345N_ζ	95.7%
O_C of 2PG	Arg374N_ε	96.4%	O_C of PEP	Arg374$N_{\eta2}$	88.7%
O_C of 2PG	Ser375N	70.2%	O_C of PEP	Arg374N_ε	18.1%
O_C of 2PG	Arg374$N_{\eta2}$	6.7%			
Chain B					
Protein-2PG			Protein-PEP		
Acceptor	Donor	Percentage	Acceptor	Donor	Percentage
Glu168$O_{\varepsilon1/\varepsilon2}$	OH of 2PG	99.4%	N/A		
OH of 2PG	Glu211$O_{\varepsilon2}$	99.4%	N/A		
O_A of 2PG	Arg374$N_{\eta2}$	69.5%	O_A of PEP	His159$N_{\varepsilon2}$	5.3%
O_B of 2PG	His159$N_{\varepsilon2}$	98.8%	O_B of PEP	Ser375O_γ	97.2%
O_B of 2PG	Ser375O_γ	91.2%	O_B of PEP	Arg374N_ε	82.1%
O_B of 2PG	Ser39N	88.7%	O_B of PEP	Ser375N	59.1%
O_B of 2PG	Ala38N	71.9%	O_C of PEP	Arg374$N_{\eta2}$	98.5%
O_B of 2PG	Ser39O_γ	5.5%	O_C of PEP	Lys345N_ζ	96.3%
O_C of 2PG	Arg374N_ε	98.3%	O_C of PEP	Arg374N_ε	5.4%
O_C of 2PG	Ser375N	55.8%			

[a]A hydrogen bond is defined to occur when the donor-acceptor distance is less than or equal to 3.0 Å, and the angle of the donor, hydrogen, and acceptor is greater than or equal to 135°. The percentage population of each hydrogen bond over the entire MD trajectory is given, and only hydrogen bonds with percentages ≥ 5% are shown. For any donor atom that can donate multiple hydrogen atoms, the hydrogen bond percentage population was calculated by summing up all possible hydrogen-bonding interactions. These analyses were carried out by using cpptraj[17] in AmberTools17.[14]

Table S6. Statistics of the loop conformations for different states of enolase obtained from crystal structures.

PDB[a]	Enzyme	State	Ligand	L1[b]	L2[c]	Ref
3ENL	Yeast enolase	E	Sulfate	Open (N/A, 2.69)	Open (6.83)	18
1EBH Chain A	Yeast enolase	E- Mg_A^{2+}	Cl^-	Open (N/A, 2.93)	Open (8.31)	19
7ENL	Yeast enolase	E-Mg_A^{2+}-L	2PG	Semi-closed (N/A, 10.24)	Open (8.01)	20
2XH2 Chain A	Yeast enolase S39N/D321A	E- Mg_A^{2+}-L	2PG	Semi-closed (N/A, 11.83)	Open (5.97)	21
2XH2 Chain B	Yeast enolase S39N/D321A	E-Mg_A^{2+}-L	2PG	Open (N/A, 3.00)	Open (6.31)	21
2XH4 Chain A	Yeast enolase S39A/D321A	E- Mg_A^{2+}-L	2PG	Semi-closed (N/A, 11.68)	Closed (2.83)	21
2XH4 Chain B	Yeast enolase S39A/D321A	E-Mg_A^{2+}-L-Mg_B^{2+}	2PG	N/A (missing 38-59)	Closed (3.73[3.03[d]]	21
2XH4 Chain D	Yeast enolase S39A/D321A	E-Mg_A^{2+}-L	2PG	N/A (missing 38-59)	Closed (3.63[2.97[d]]	21
1NEL	Yeast enolase	E- Mg_A^{2+}-L	Phos-phate and F^-	Semi-closed (N/A, 10.94)	Closed (2.66)	22
5ENL	Yeast enolase	E-Ca_A^{2+}-L	2PG	Open (N/A, 2.67)	Open (6.09)	20
6ENL	Yeast enolase	E-Zn_A^{2+}-L	PGA[e]	Open (N/A, 2.49)	Open (6.44)	20
2AKM Chain B	Human neuronal enolase	E-Mg_A^{2+}-L	Phos-phate	Semi-closed (N/A, 10.33)	Closed (3.75)	23
1ONE Chain A	Yeast enolase	E-Mg_A^{2+}-L-Mg_B^{2+}	2PG /PEP	Closed (3.57, 11.32)	Closed (3.16/3.08)	1
2AL1 Chain A	Yeast enolase	E-Mg_A^{2+}-L-Mg_B^{2+}	2PG	Closed (3.66, 11.16)	Closed (2.91)	24
2AL1 Chain B	Yeast enolase	E-Mg_A^{2+}-L-Mg_B^{2+}	PEP	Closed (3.50, 11.24)	N/A (missing 158-162)	24
2AL2 Chain A	Yeast enolase K345A	E-Mg_A^{2+}-L-Mg_B^{2+}	2PG/ PEP	Closed (3.42, 11.25)	Closed (2.67/3.0)	24
2AL2 Chain B	Yeast enolase N80D/N126D	E-Mg_A^{2+}-L-Mg_B^{2+}	2PG/ PEP	N/A (missing 39, 11.17)	N/A (missing 158-162)	24
2PU0	Trypanosoma brucei enolase	E-Zn_A^{2+}-L-Zn_B^{2+}	PhAH[f]	Closed (3.54, 11.47)	Closed (3.0)	25

Table S6. (Continued)

PDB[a]	Enzyme	State	Ligand	L1[b]	L2[c]	Ref
2PTZ	Trypanosoma brucei enolase	E-Zn_A^{2+}-L-Zn_B^{2+}	PhAH	Closed (3.40, 11.31)	Open (9.90)	25
1ELS	Yeast enolase	E-Mn_A^{2+}-L-Mn_B^{2+}	PhAH	Semi-closed (4.83, 10.52)	Open (6.08)	26
2PTY	Trypanosoma brucei enolase	E-Zn_A^{2+}-L-Zn_B^{2+}	PEP	Closed (3.55, 11.70)	Closed (2.90)	25
2ONE Chain A	Yeast enolase	E-Mg_A^{2+}-L-Li_B^{+}	2PG	Closed (3.93, 11.69)	Closed (3.24)	27
2ONE Chain B	Yeast enolase	E-Mg_A^{2+}-L-Li_B^{+}(?)[g]	PEP	Closed (N/A, 11.93)	Open (6.87)	27
1L8P Chain A	Yeast enolase S39A	E-Mg_A^{2+}-L-Mg_B^{2+}	PhAH	Semi-open (6.08, 11.72)	Open (5.50)	28
2AKZ Chain A	Human neuronal enolase	E-Mg_A^{2+}-L-Mg_B^{2+}	Phos-phate and F^-	Closed (3.49, 11.20)	Closed (2.93)	23
2AKM Chain A	Human neuronal enolase	E-Mg_A^{2+}-L-Mg_B^{2+}	Phos-phate	Closed (3.57, 11.81)	Closed (2.96)	23
2XH0 Chain A	Yeast enolase S39N/Q157K/ D321R	E-Mg_A^{2+}-L	PEP	Semi-closed (N/A, 11.64)	Open (8.32)	21
2XGZ Chain A	Yeast enolase S39N/D321R	E- Mg_A^{2+}-L	PEP	Semi-Closed (N/A, 11.48)	N/A (missing 159 sidechain)	21
2XGZ Chain B	Yeast enolase S39N/D321R	E- Mg_A^{2+}-L	PEP	Open (N/A, 2.82)	Open (5.06)	21

[a]Some structures are shown with selected chains because other chains have similar loop conformations.

[b]The first value in parentheses is the distance between Mg_B^{2+} and Ser39C_α, and the second value in parentheses is the distance between Ala38O and Glu47N, where N/A denotes not available. Enolases other than yeast enolase may have different residue numbers for these residues, and these differences were considered in the current table.

[c]The number in the parentheses is the distance between the His159$N_{\varepsilon 2}$ and the closest oxygen atom in the phosphate/sulfate group of the ligand or the Cl^- ion. Enolases other than yeast enolase may have different residue numbers for these residues, and these differences were considered in the current table.

[d]The number in the brackets by considering correction of the His orientation.

[e]Abbreviation for 2-phosphoglycolic acid.

[f]Abbreviation for phosphonoacetohydroxamate, which is a mimic of the transition state.

[g]Because of the partially disordered Ser39, the authors were not able to determine the presence of the Li_B^+ ion.

Table S7. Average number of hydrogen bonds involving L1 or the ligand for the closed loop and open loop states of the protein-2PG and protein-PEP systems[a]

	Protein-2PG		Protein-PEP	
	Closed loop	Open loop	Closed loop	Open loop
Internal to L1	0.4	0.4	0.1	0.0
L1 (D) and other residues (A)	3.6	3.1	4.9	2.5
L1 (A) and other residues (D)	1.3	0.6	0.7	1.9
L1 (D) and solvent (A)	2.3	4.0	2.8	4.7
L1 (A) and solvent (D)	6.5	10.0	7.1	8.8
L1 (D) and 2PG/PEP (A)	1.8	0.0	0.1	0.0
L1 (A) and 2PG/PEP (D)	0.0	0.0	0.0	0.0
Total involving L1	16.0	18.2	15.7	17.9
Internal to 2PG/PEP	0.0	1.0[b]	0.0	0.0
2PG/PEP (D) and protein (A)	1.0	0.0	0.0	0.0
2PG/PEP (A) and protein (D)	8.1	4.7	6.3	3.9
2PG/PEP (D) and solvent (A)	0.0	0.0	0.0	0.0
2PG/PEP (A) and solvent (D)	0.0	3.4	0.1	2.7
Total involving 2PG/PEP	9.0	9.1	6.5	6.6

[a]A hydrogen bond is defined to occur when the donor-acceptor distance is less than or equal to 3.0 Å and the angle of the donor, hydrogen, and acceptor is greater than or equal to 135°. In the table, D and A denote donor and acceptor, respectively. Snapshots from representative windows within the umbrella sampling simulations were used for these analyses, as stated in Part D of the protocol for umbrella sampling in this SI. These analyses were carried out by using cpptraj[17] in AmberTools17.[14] [b]The internal hydrogen bond between the hydroxyl group and phosphate group in 2PG.

Table S8. Percentage population of hydrogen bonds involving hydroxyl group of 2PG in the closed loop and open loop states[a]

Acceptor	Donor	Closed loop state	Open loop state
Glu168$O_{\varepsilon 1/\varepsilon 2}$	OH of 2PG	97.9%	N/A
$O_{A/B/C}$ of 2PG	OH of 2PG	N/A	99.8%
OH of 2PG	Glu211$O_{\varepsilon 2}$	99.5%	87.7%

[a]A hydrogen bond is defined to occur when the donor-acceptor distance is less than or equal to 3.0 Å, and the angle of the donor, hydrogen, and acceptor is greater than or equal to 135°. The percentage population of each hydrogen bond is given, and only hydrogen bonds with percentages ≥ 5% are shown. Snapshots from representative windows within the umbrella sampling simulations were used for these analyses, as stated in Part D of the protocol for umbrella sampling in this SI. These analyses were carried out by using cpptraj[17] in AmberTools17.[14]

References

1. Larsen, T. M.; Wedekind, J. E.; Rayment, I.; Reed, G. H., A Carboxylate Oxygen of the Substrate Bridges the Magnesium Ions at the Active Site of Enolase: Structure of the Yeast Enzyme Complexed with the Equilibrium Mixture of 2-Phosphoglycerate and Phosphoenolpyruvate at 1.8 Å Resolution. *Biochemistry* **1996,** *35*, 4349-4358.
2. Gordon, J. C.; Myers, J. B.; Folta, T.; Shoja, V.; Heath, L. S.; Onufriev, A., H++: A Server for Estimating Pkas and Adding Missing Hydrogens to Macromolecules. *Nucleic Acids Res.* **2005,** *33*, W368-W371.
3. Frisch, M. J.; Trucks, G. W.; Schlegel, H. B.; Scuseria, G. E.; Robb, M. A.; Cheeseman, J. R.; Scalmani, G.; Barone, V.; Mennucci, B.; Petersson, G. A.; Nakatsuji, H.; Caricato, M.; Li, X.; Hratchian, H. P.; Izmaylov, A. F.; Bloino, J.; Zheng, G.; Sonnenberg, J. L.; Hada, M.; Ehara, M.; Toyota, K.; Fukuda, R.; Hasegawa, J.; Ishida, M.; Nakajima, T.; Honda, Y.; Kitao, O.; Nakai, H.; Vreven, T.; Jr., J. A. M.; Peralta, J. E.; Ogliaro, F.; Bearpark, M.; Heyd, J. J.; Brothers, E.; Kudin, K. N.; Staroverov, V. N.; Keith, T.; Kobayashi, R.; Normand, J.; Raghavachari, K.; Rendell, A.; Burant, J. C.; Iyengar, S. S.; Tomasi, J.; Cossi, M.; Rega, N.; Millam, J. M.; Klene, M.; Knox, J. E.; Cross, J. B.; Bakken, V.; Adamo, C.; Jaramillo, J.; Gomperts, R.; Stratmann, R. E.; Yazyev, O.; Austin, A. J.; Cammi, R.; Pomelli, C.; Ochterski, J. W.; Martin, R. L.; Morokuma, K.; Zakrzewski, V. G.; Voth, G. A.; Salvador, P.; Dannenberg, J. J.; Dapprich, S.; Daniels, A. D.; Farkas, O.; Foresman, J. B.; Ortiz, J. V.; Cioslowski, J.; Fox, D. J. *Gaussian 09, Revision D. 01*, Gaussian Inc.: Wallingford, CT, 2013.
4. Case, D. A.; Cheatham, T. E.; Darden, T.; Gohlke, H.; Luo, R.; Merz Jr, K. M.; Onufriev, A.; Simmerling, C.; Wang, B.; Woods, R. J., The Amber Biomolecular Simulation Programs. *J. Comput. Chem.* **2005,** *26*, 1668-1688.
5. Jorgensen, W. L.; Chandrasekhar, J.; Madura, J. D.; Impey, R. W.; Klein, M. L., Comparison of Simple Potential Functions for Simulating Liquid Water. *J. Chem. Phys.* **1983,** *79*, 926-935.
6. Li, P.; Roberts, B. P.; Chakravorty, D. K.; Merz Jr, K. M., Rational Design of Particle Mesh Ewald Compatible Lennard-Jones Parameters for +2 Metal Cations in Explicit Solvent. *J. Chem. Theory Comput.* **2013,** *9*, 2733-2748.
7. Li, P.; Song, L. F.; Merz Jr, K. M., Systematic Parameterization of Monovalent Ions Employing the Nonbonded Model. *J. Chem. Theory Comput.* **2015,** *11*, 1645-1657.
8. Maier, J. A.; Martinez, C.; Kasavajhala, K.; Wickstrom, L.; Hauser, K. E.; Simmerling, C., Ff14sb: Improving the Accuracy of Protein Side Chain and Backbone Parameters from Ff99sb. *J. Chem. Theory Comput.* **2015,** *11*, 3696-3713.
9. Darden, T.; York, D.; Pedersen, L., Particle Mesh Ewald: An N□Log(N) Method for Ewald Sums in Large Systems. *J. Chem. Phys.* **1993,** *98*, 10089-10092.
10. Ryckaert, J.-P.; Ciccotti, G.; Berendsen, H. J., Numerical Integration of the Cartesian Equations of Motion of a System with Constraints: Molecular Dynamics of N-Alkanes. *J. Comput. Phys.* **1977,** *23*, 327-341.
11. Miyamoto, S.; Kollman, P. A., Settle: An Analytical Version of the Shake and Rattle Algorithm for Rigid Water Models. *J. Comput. Chem.* **1992,** *13*, 952-962.
12. Salomon-Ferrer, R.; Götz, A. W.; Poole, D.; Le Grand, S.; Walker, R. C., Routine Microsecond Molecular Dynamics Simulations with Amber on Gpus. 2. Explicit Solvent Particle Mesh Ewald. *J. Chem. Theory Comput.* **2013,** *9*, 3878-3888.
13. Case, D. A.; Betz, R. M.; Botello-Smith, W.; Cerutti, D. S.; Cheatham, I. T. E.; Darden, T. A.; Duke, R. E.; Giese, T. J.; Gohlke, H.; Goetz, A. W.; Homeyer, N.; Izadi, S.; Janowski, P.; J.

Kaus, A.; Kovalenko; Lee, T. S.; LeGrand, S.; Li, P.; Lin, C.; Luchko, T.; Luo, R.; Madej, B.; Mermelstein, D.; Merz, K. M.; Monard, G.; Nguyen, H.; Nguyen, H. T.; Omelyan, I.; Onufriev, A.; Roe, D. R.; Roitberg, A.; Sagui, C.; Simmerling, C. L.; Swails, J.; Walker, R. C.; Wang, J.; Wolf, R. M.; Wu, X.; Xiao, L.; Kollman, P. A. *Amber 2016*, University of California, San Francisco.: 2016.
14. Case, D. A.; Cerutti, D. S.; T. E. Cheatham, I.; Darden, T. A.; Duke, R. E.; Giese, T. J.; Gohlke, H.; Goetz, A. W.; Greene, D.; Homeyer, N.; Izadi, S.; Kovalenko, A.; Lee, T. S.; LeGrand, S.; Li, P.; Lin, C.; Liu, J.; Luchko, T.; Luo, R.; Mermelstein, D.; Merz, K. M.; Monard, G.; Nguyen, H.; Omelyan, I.; Onufriev, A.; Pan, F.; Qi, R.; Roe, D. R.; Roitberg, A.; Sagui, C.; Simmerling, C. L.; Botello-Smith, W. M.; Swails, J.; Walker, R. C.; Wang, J.; Wolf, R. M.; Wu, X.; Xiao, L.; York, D. M.; Kollman, P. A. *Amber 2017*, University of California, San Francisco: 2017.
15. Chakravorty, D. K.; Li, P.; Tran, T. T.; Bayse, C. A.; Merz Jr, K. M., Metal Ion Capture Mechanism of a Copper Metallochaperone. *Biochemistry* **2016,** *55*, 501-509.
16. Grossfield, A., "WHAM: The Weighted Histogram Analysis Method", Version 2.0.9.1; available via the Internet at: http://membrane.urmc.rochester.edu/wordpress/?page_id=126 (accessed Dec 20, 2017).
17. Roe, D. R.; Cheatham III, T. E., Ptraj and Cpptraj: Software for Processing and Analysis of Molecular Dynamics Trajectory Data. *J. Chem. Theory Comput.* **2013,** *9*, 3084-3095.
18. Stec, B.; Lebioda, L., Refined Structure of Yeast Apo-Enolase at 2.25 Å Resolution. *J. Mol. Biol.* **1990,** *211*, 235-248.
19. Wedekind, J. E.; Reed, G. H.; Rayment, I., Octahedral Coordination at the High-Affinity Metal Site in Enolase: Crystallographic Analysis of the Mgii-Enzyme Complex from Yeast at 1.9. Ang. Resolution. *Biochemistry* **1995,** *34*, 4325-4330.
20. Lebioda, L.; Stec, B., Mechanism of Enolase: The Crystal Structure of Enolase-Magnesium-2-Phosphoglycerate/Phosphoenolpyruvate Complex at 2.2-. Ang. Resolution. *Biochemistry* **1991,** *30*, 2817-2822.
21. Schreier, B.; Höcker, B., Engineering the Enolase Magnesium Ii Binding Site: Implications for Its Evolution. *Biochemistry* **2010,** *49*, 7582-7589.
22. Lebioda, L.; Zhang, E.; Lewinski, K.; Brewer, J. M., Fluoride Inhibition of Yeast Enolase: Crystal Structure of the Enolase–Mg2+–F−–Pi Complex at 2.6 Å Resolution. *Proteins* **1993,** *16*, 219-225.
23. Qin, J.; Chai, G.; Brewer, J. M.; Lovelace, L. L.; Lebioda, L., Fluoride Inhibition of Enolase: Crystal Structure and Thermodynamics. *Biochemistry* **2006,** *45*, 793-800.
24. Sims, P. A.; Menefee, A. L.; Larsen, T. M.; Mansoorabadi, S. O.; Reed, G. H., Structure and Catalytic Properties of an Engineered Heterodimer of Enolase Composed of One Active and One Inactive Subunit. *J. Mol. Biol.* **2006,** *355*, 422-431.
25. Marcos, V.; Dias, S. M. G.; Mello, L. V.; da Silva Giotto, M. T.; Gavalda, S.; Blonski, C.; Garratt, R. C.; Rigden, D. J., Structural Flexibility in Trypanosoma Brucei Enolase Revealed by X‐Ray Crystallography and Molecular Dynamics. *FEBS J.* **2007,** *274*, 5077-5089.
26. Zhang, E.; Hatada, M.; Brewer, J. M.; Lebioda, L., Catalytic Metal Ion Binding in Enolase: The Crystal Structure of an Enolase-Mn2+-Phosphonoacetohydroxamate Complex at 2.4-. Ang. Resolution. *Biochemistry* **1994,** *33*, 6295-6300.
27. Zhang, E.; Brewer, J. M.; Minor, W.; Carreira, L. A.; Lebioda, L., Mechanism of Enolase: The Crystal Structure of Asymmetric Dimer Enolase− 2-Phospho-D-Glycerate/Enolase− Phosphoenolpyruvate at 2.0 Å Resolution. *Biochemistry* **1997,** *36*, 12526-12534.

28. Poyner, R. R.; Larsen, T. M.; Wong, S.-W.; Reed, G. H., Functional and Structural Changes Due to a Serine to Alanine Mutation in the Active-Site Flap of Enolase. *Arch. Biochem. Biophys.* **2002,** *401*, 155-163.